INTL JOURNAL OF ELECTRONICS AND TELECOMMUNICATIONS, 2025, VOL. 71, NO. 3, PP. 1-7
Manuscript received December 5, 2024; revised July 2025. doi: 10.24425/ijet.2025.153626

BLE phase-based ranging: accuracy and capability under strong Wi-Fi interference

Igor Kravets, Nazarii Kotliar, Oleksandr Karpin, and Andriy Luchechko

Abstract—**Indoor positioning and asset tracking have become popular and essential for different applications and use cases. Many systems use Bluetooth Low Energy (BLE) wireless personal area network technology for communication and ranging purposes. Unfortunately, due to limitations of the ISM radio band, other communication technologies such as Z-Wave, ZigBee, and Wi-Fi also use the same frequency bandwidth. This overlap often leads to interference that affects the performance of BLE systems. This work evaluates the effect of Wi-Fi interference on the phase-based ranging distance estimate for different BLE to Wi-Fi signal power ratios. We show the random distance error increasing more than 3 times for both Inverse Fourier Transform and Multiple Signal Classification algorithms at short distances. Based on simulation results and infield experiments, we identified that the interference becomes marginal for distances more than 10m, and the device can't identify the location correctly in case of similar Wi-Fi and BLE Tx power. In the case of long-distance ranging, ignoring interfered frequencies improves the situation dramatically, but this results in worse resolution and sometimes may identify the distance incorrectly due to false peaks.**

Keywords—**BLE Phase-Based Ranging; Distance Estimation; Wi-Fi Interference; Inverse Furrier Transform; Multiple Signal Classification**

I. Introduction

THE Internet of Things (IoT) is becoming increasingly popular nowadays. Projections suggest that the number of IoT devices will reach 50 billion within the next decade [1]. This growth is mainly caused by the availability of cheap narrow-band systems such as Bluetooth Low Energy (BLE) and Zigbee, which are widely used in industries including healthcare, fitness, beacons, security, and home entertainment [2]. The basic requirement for these applications is the ability to estimate the distance between two devices, which later can be used for localization purposes. Although ultra-wideband (UWB) systems provide better-ranging accuracy compared to narrow-band systems, UWB usage in IoT is rather limited systems due to higher cost [3].

The distance between the two radio systems can be estimated based on the various approaches, including Received Signal Strength Indicator (RSSI), Time-of-flight (ToF)/Time-difference-of-arrival (TDoA), and Phase-Based Ranging (PBR). RSSI-based ranging suffers from low accuracy [4],[5] and, in practice, requires a large number of devices and specialized antenna designs to minimize ground reflections. ToF systems using BLE technology provide poor distance estimates even in open spaces [6] TDoA is the most appropriate for the UWB systems, where the bandwidth and, hence, time resolution are high [7]. For narrow-band systems such as BLE and ZigBee, phase-based ranging is considered the most effective [8],[9].

In phase-based ranging, the channel is measured between two devices – initiator and reflector – on a uniform frequency sequence over the desired bandwidth [8]. These measurements can be processed using the Inverse Discrete Fourier Transform (IDFT) [10] to obtain the Channel Impulse Response (CIR). However, in a multipath environment where signals may take multiple paths to reach the receiver, the accuracy of this method is limited due to the resolution of the IDFT [11]. In this case, instead of FFT, super-resolution algorithms such as Multiple Signal Classification (MUSIC) can be used to enhance the accuracy of ranging in multipath environments [12].

The advantage of the MUSIC algorithm application on the phase-based ranging consists in its ability to resolve signal and noise spaces and, in such a way, increase the ranging resolution [11]. Unfortunately, due to the multipath nature, the signal space is compressed into one signal due to the total correlation between Line-of-Sight (LoS) and other reflected rays. To decorrelate signals, the spatial smoothing technique must be used, which requires In phase and Quadrature (IQ) measurements at the initiator and reflector taken on a uniform, frequency domain sampling grid [11]. However, this assumption is violated because some channels are reserved for Bluetooth advertising packets, and the other channels interfere with Bluetooth, Zigbee, or WIFI signals, which use the same bandwidth [13]. Without the spatial smoothing technique, MUSIC shows performance identical to DFT. Thus, both methods are still used.

To the best of our knowledge, there is no work in literature, which evaluates Wi-Fi noise effect on accuracy of phase-based ranging in multipath environments. In this paper, we investigate the robustness and limitations of the BLE phase-based ranging solution, which uses whole 2.4GHz BLE ISM radio bandwidth. The first section describes the principle of phase-based ranging. In the second section, we discuss spectral distance estimation using IFT and MUSIC. In the third section we evaluate the accuracy of distance determination under intense Wi-Fi noise and estimate the limitation of distance measuring by this methodology.

I. Kravets, O. Karpin, A. Luchechko are with Department of Sensor and Semiconductor Electronics, Ivan Franko National University of Lviv, Ukraine, and also are with Infineon Technologies, Ukraine (e-mail: dr.kravets@gmail.com, Oleksandr.Karpin@infineon.com, andriy.luchechko@lnu.edu.ua).

N. Kotliar is with Infineon Technologies, Ukraine, and also is with the Department of Telecommunications, Lviv Polytechnic National University, Ukraine (e-mail: nazarii.kotliar@gmail.com).

II. PHASE-BASED RANGING

Phase-Based Ranging (PBR) method involves the measurement of IQ components at several frequencies [8],[9]. Both the initiator and reflector transmit and receive harmonic signals (tones) at each frequency, enabling the measurement of phase and magnitude using quadrature demodulation [14]. This paper discusses IQ measurements conducted on both the initiator and the reflector sides.

Assume the initiator and reflector are spaced apart from each other at distance d. If the initiator transmits a tone given by:

$$S_0^i(t) = A_0^i e^{j\cdot 2\pi f_1 (t+\varphi_0)} \tag{1}$$

where A_0^i is the transmitted magnitude and φ_0 is the transmitted phase. The tone at the reflector at frequency f_1 can be described by the following equation:

$$S_1^r(t) = A_1^r e^{j\cdot 2\pi f_1 (t - {d}/{c} + \varphi_1)}, \tag{2}$$

where A_1^r is the measured amplitude of the tone, t is time, and c is the speed of light. The reflector returns the signal after a known time delay Δt. Then initiator receives the signal:

$$\widehat{S_1^i}(t) = \widehat{A_1^i} e^{j\cdot 2\pi f_1 (t - {d}/{c} + \varphi_1 - \Delta t - {d}/{c})}. \tag{3}$$

We can evaluate the IQ signal change caused by the distance at the initiator for frequency f_1:

$$IQ_1 = \frac{\widehat{S_1^i}(t)}{S_0^i(t)} = \frac{\widehat{A_1^i}}{A_1^i} e^{-j\cdot 2\pi f_1 ({2d}/{c} + \Delta t)}. \tag{4}$$

After substitution $A_1 = \frac{\widehat{A_1^i}}{A_1^i} e^{-j\cdot 2\pi f_1 \Delta t}$, we obtain the IQ change for all frequencies:

$$IQ_1 = A_1 e^{-j\cdot 2\pi f_1 {2d}/{c}}, \tag{5}$$

$$IQ = [IQ_1, IQ_2, \dots, IQ_n], \tag{6}$$

$$IQ = \left[A_1 e^{-j\cdot 2\pi f_1 {2d}/{c}}, A_2 e^{-j\cdot 2\pi f_2 {2d}/{c}}, \dots, A_n e^{-j\cdot 2\pi f_n {2d}/{c}}\right], \tag{7}$$

It can be observed that the main information about the distance is hidden in the phase component of IQs and it has the linear dependency on the distance [9]:

$$d \sim \sum_2^n \Delta\varphi_n\,,\ \Delta\varphi_n = \arg(IQ_n) - \arg(IQ_{n-1}), \tag{8}$$

$$d = \frac{c}{4\pi} \cdot \frac{\sum_2^n \Delta\varphi_n}{\Delta f \cdot (n-1)}, \tag{9}$$

where Δf is the frequency step. Ideally, function $\varphi = g(f)$ should be a straight line, whose is proportional to the distance between the initiator and reflector. However, in practice, this dependency will not be linear due to the noise and complicated environment, which can increase measurement error [15].

B. BLE PBR using IFT

Inverse Furrier Transform (IFT) is one of the spectral methods that can be used to convert the transfer function into an impulse response [10]. For random sampling, a modified Furrier Transform for non-equispaced data is recommended [16]. After the impulse response is estimated, the extreme values arguments represent the delays of the rays, which correspond to distances in our case.

Assume the transfer function H_n is a set of complex numbers, unevenly discretized at frequency points f_n, where $n = 1 \dots N$. The impulse response h_k for any given moment of time t_k can be estimated using the modified Inverse Furrier Transform:

$$\hat{h}_k^{(1)} = \sum_1^N X_n \cdot exp(j \cdot 2\pi \cdot f_n t_k)\,. \tag{10}$$

Hence, for the sequence of measured IQ data, IQ_n with length N, which is related to the number of scanned frequencies f_n, to convert it into an impulse response with the set of distance values $2d_k$, equation (10) can be transformed as follows:

$$\hat{h}_k^{(1)} = \sum_1^N IQ_n \cdot exp\left(j \cdot 2\pi \cdot \frac{2d_k}{c} f_n\right), \tag{11}$$

where c is the speed of light. A similar dependency can be obtained using the correlation method [17].

The main advantage of the Inverse Fourier Transform is its ability to relate the peak value of a lobe to the signal power at a specific distance. In addition, this white noise does not almost affect the main lobe's position as it is distributed uniformly among all the frequencies. The disadvantage of this method is the quite wide lobes caused by the limited number of scanned frequencies (up to 80 frequencies in the BLE range). Therefore, the identification of close ray path distances is challenging.

In Figure 1, we can observe a sample of the normalized IFT calculation based on non-equispaced equations. Synthetic IQ data was generated as input. However, unlike phase-based ranging due to which data from the initiator and reflector is combined, in this example only the pure environment transfer function was used, which consists of two rays – 15m and 20m, with the latter having twice lower magnitude than the first one. Otherwise, the pseudospectrum could transform into three lobes: two mentioned rays and "ghost" resulting from their combination, potentially doubling the perceived distances due to the two-sided measurement. The location of the maximums of these lobes refers to the actual distance values.

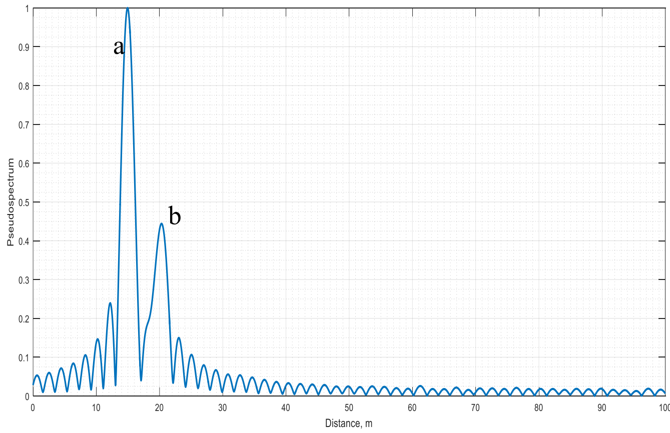

Fig.1 IFT pseudospectrum calculated for IQ data with two rays: (a) – 15m, (b) – 20m

C. BLE PBR with high resolution

The MUltiple SIgnal Classification (MUSIC) algorithm is a sub-spaced method, predominantly used for estimating the Angle of Arrival (AoA), or two dimensional Direction of Arrival (DoA) and Dirrectoin of Departure (DoD) for radars, but it also can be adapted for distance estimation [12], [18], [19].

Assume the IQ values at N frequencies are measured in an environment characterized by M rays with different distances d_m, but $M < N$. The true IQ values can be calculated as follows:

$$IQ_n = \sum_1^M iq_m \cdot exp\left(-j \cdot 2\pi f_n \cdot \frac{2d_m}{c}\right), \tag{12}$$

where

$$iq_M = A_M \cdot exp\,(-j\varphi_M)\,. \tag{13}$$

The sequence of N- measured IQ values can be expressed as:

$$IQ = [IQ_1, IQ_2, \dots, IQ_N]^T + n = S \cdot iq + n, \qquad (14)$$

where $\vec{n}$ is the measurement noise sequence, $\overrightarrow{iq}$ is the sequence of complex magnitudes:

$$iq = [iq_1, iq_2, \dots, iq_M]^T, \qquad (15)$$

and S is the matrix of steering vectors:

$$S = [s(d_1), s(d_2), \dots, s(d_M)], \qquad (16)$$

with each steering vector defined as:

$$s(d) = \left[e^{-j\cdot 2\pi f_1 \cdot \frac{2d}{c}}, e^{-j\cdot 2\pi f_2 \cdot \frac{2d}{c}}, \dots, e^{-j\cdot 2\pi f_N \cdot \frac{2d}{c}}\right]^T, \qquad (17)$$

These steering vectors represents the phase change of IQ values dependency at one particular distance through the N frequencies, so there are M steering vectors.

The covariance matrix of IQ sequence can be represented as:

$$R = E[IQ \cdot IQ^H] = E\left[S \cdot iq^H iq \cdot \vec{S}^H\right] + E[nn^H] = \\ = R_S + \sigma^2 I \qquad (18)$$

where R_S is the signal covariance matrix, σ is the measurement noise standard deviation, and I is the identity matrix. That is matrix R can be defined through its eigenvectors and eigenvalues:

$$R = Q(\zeta + \sigma^2 I)Q^H, \qquad (19)$$

where $\zeta = \lambda I$, $\lambda = [\lambda_1, \lambda_2, \dots, \lambda_N]$. In the case of M uncorrelated rays, we observe M non-zero eigenvalues: $\lambda_k \neq 0$, for $k \leq M$, which describe uncorrelated signal powers, and N-M zero eigenvalues: $\lambda_k = 0$, for $k > M$, describe measurement noise power.

Every eigenvalue magnitude describes the power of the corresponding signal component, and eigenvalues of matrix R are described as follows:

$$\zeta + \sigma^2 I = \begin{bmatrix} \lambda_1 + \sigma^2 & 0 & \cdots & 0 \\ 0 & & & \\ \vdots & \ddots & \cdots & \vdots \\ \vdots & \cdots & \lambda_M + \sigma^2 & \vdots \\ & & \ddots & \\ 0 & 0 & \cdots & \sigma^2 \end{bmatrix}, \qquad (20)$$

Thus, the MUSIC algorithm estimates impulse response for distance testing as:

$$\hat{h}_k^{(2)} = (s(d_V)^H Q_n Q_n^H s(d_V))^{-1}, \qquad (21)$$

where Q_n are the noise eigenvectors. MUSIC provides good pseudospectrum estimates with local maximums in the locations of ray delays because the steering vector $s(d)$, responsible for the true distance and noise eigenvectors Q_n are orthogonal. This means MUSIC can provide enhanced spectral resolution through the separation of signal and noise spaces.

However, for BLE phase-based ranging, the MUSIC impulse response estimate $\hat{h}_k^{(2)}$ shows no significant advantage over the IFT estimate $\hat{h}_k^{(1)}$ due to the complete correlation between reflected waves. Thus, there is only one uncorrelated signal source and *M=1*.

The covariance matrix R, defined by its eigenvalues $\lambda \epsilon Re$ and Q is a matrix, whose columns are eigenvectors of R, satisfy the equation:

$$I = QQ^H, \qquad (22)$$

where I is the identity matrix. Rewriting the denominator in equation (8):

$$s(d_k)^H Q_n Q_n^H s(d_k) = I - s(d_k)^H Q_s Q_s^H s(d_k) = \\ = I - s(d_k)^H Q_s Q_s^H s(d_k) = I - (s(d_k)^H Q_s)^2. \qquad (23)$$

Considering that $s(d_k)^H Q_s = \hat{h}_k^{(1)}$, we obtain:

$$\hat{h}_k^{(2)} = \frac{1}{I - \left(\hat{h}_k^{(1)}/\lambda_{max}\right)^2}, \qquad (24)$$

where Q_n are noise-related eigenvectors, Q_s is the signal eigenvector, λ_{max} is the dominant eigenvalue of the covariance matrix R. The last equation indicates that MUSIC and IFT are mutually connected in the case of M=1, and their extremes have identical argument.

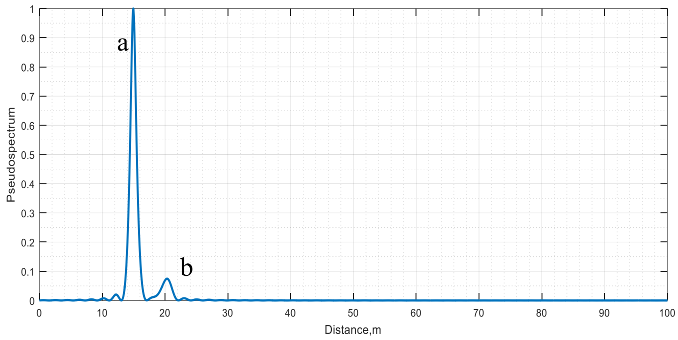

Fig.2 MUSIC pseudospectrum calculated for IQ data with two rays: (a) – 15m, (b) – 20m

In Figure 2 we observe the example of MUSIC pseudospectrum calculated for the exact same IQ data given in Figure 1. Unlike IFT, the relation between lobes' heights has no physical meaning, but the maximums are located at the same distance points as previously described.

To achieve super-resolution in MUSIC pseudospectrum and advantage over IFT transform, we should decorrelate our rays in the BLE channel. One of the possible ways to do this is to use the spatial smoothing algorithm [20]. In general, it is the moving average of a matrix with size N-K, where K is the smoothing order along the main diagonal of the covariance matrix R. For phase-based ranging, we would have $M = 2P + 1$, where P is the number of rays, M is the number of the dominant eigenvalues. An example of smoothing algorithm is demonstrated in Fig. 3. The impulse response consists of two close distances, 20 and 25 meters. Without the smoothing, the estimated impulse response consists of one dominant extreme with an incorrect argument. However, after applying spatial smoothing to the covariance matrix, two peaks emerge with accurate arguments, clearly distinguishing close distances.

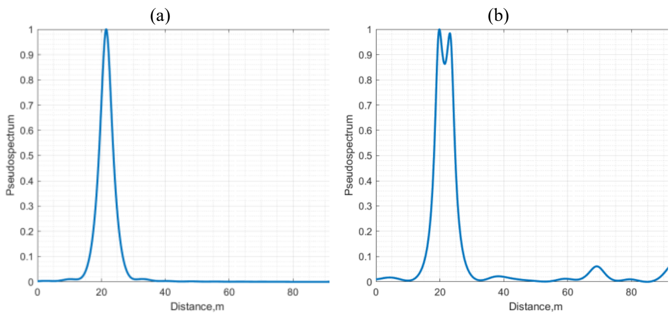

Fig.3 Example of MUSIC pseudospectrum without (a) and with (b) spatial smoothing for two close distances

III. BLE PBR UNDER STRONG WI-FI INTERFERENCE

To estimate the influence of Wi-Fi interference on the BLE Phase-Based Ranging, we set up an experiment using two NXP KW38 boards and a TP-Link TL-WR841N Wi-Fi router. Additionally, two PCs were used to control boards and Wi-Fi router parameters, such as channel and bitrate, and to control the communication intensity of data transfer via Wi-Fi.

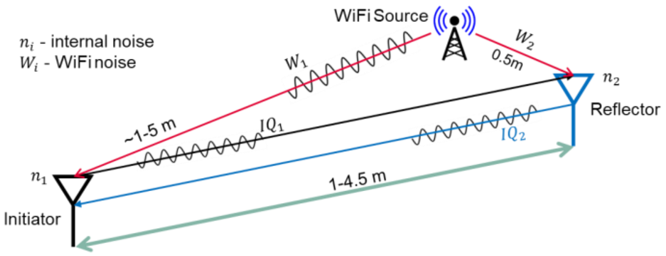

Fig.4 Schematics of experiment

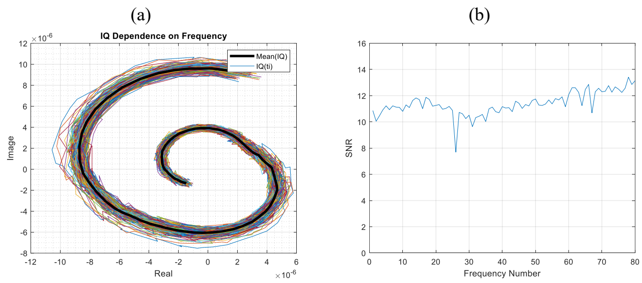

Fig. 5. a) - Samples of IQ values represented in Nyquist plot; b) SNR at each frequency

Initially, to receive close to ideal results (reference result), a sequence of 400 measurements at 80 BLE frequencies at a fixed distance with the turned-off Wi-Fi source were carried out (Fig. 4). The distances were then calculated using IFT and MUSIC methods. Here, we demonstrate only the IFT result because both methods provide similar pseudo-spectrums with identical extremes location due to a significant thermal noise floor.

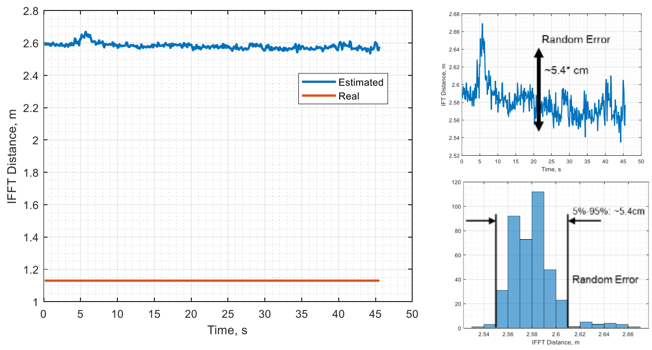

Fig. 6. Distance estimation result via IFT

The mean distance value was 2.58 m and random 90% peak-to-peak error of 5.4 cm. Some bias error (Fig. 6) was present, caused by the multipath effects, analogue time delays in devices, and transfer function of the radio channels and antennas.

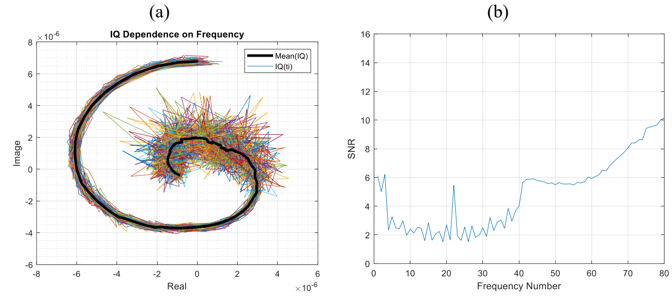

Fig. 7. a) - Samples of IQ values represented in Nyquist plot under Wi-Fi noise; b) - SNR at each frequency under Wi-Fi noise

Without changing the position of the initiator, reflector, and Wi-Fi noise sources, the data transmission process via Wi-Fi was set with a 40 Mbps bitrate at the 1st Wi-Fi channel. It covers the frequencies approximately from 2402 MHz to 2440 MHz (Fig. 7).

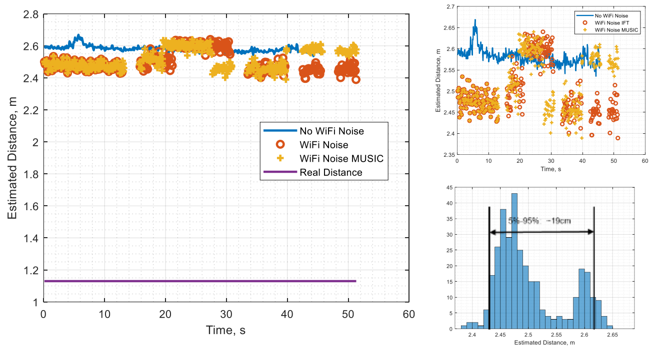

Fig. 8. Distance estimating result under Wi-Fi noise for IFT and MUSIC

This configuration resulted in a significant decrease in the total SNR, with SNR values near 2 at frequencies that interfered with Wi-Fi. The distance estimation result has changed as well. While some points are the same for MUSIC and IFT, others vary significantly. The random error increased by almost fourfold to 18.4 cm for IFT and to 17.7 cm for MUSIC. It was expected that MUSIC would have better results because of higher resistance to noise. Overall, the error is not huge because the Wi-Fi communication behaves like white noise with high amplitude in the BLE radio spectrum (Fig. 8).

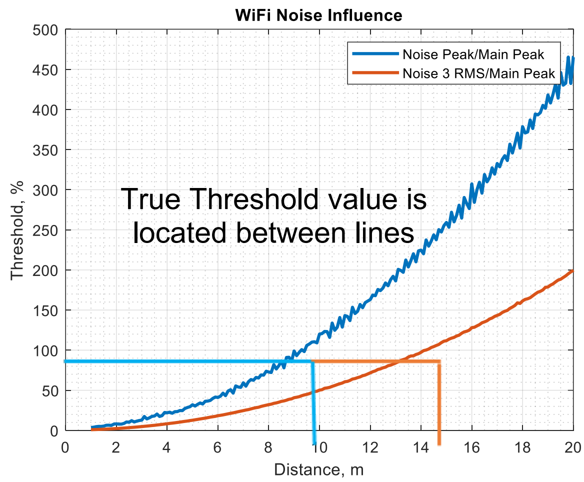

Fig. 9. Simulation result for Wi-Fi noise influence on distance estimation, calculated using IFT

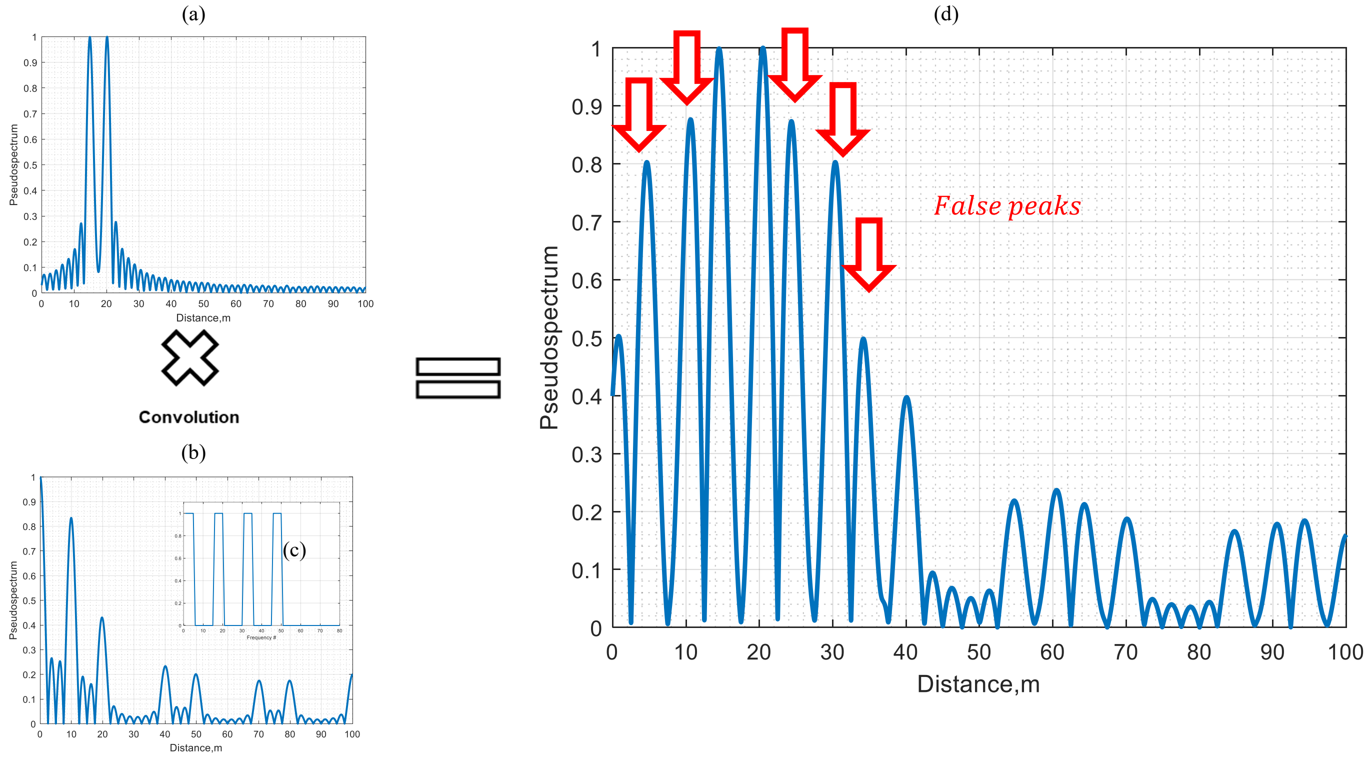

Fig. 12. Example of IFT of the IQ data with some gap pattern: (a) – IFT pseudospectrum result for two distances (15m, 20m), (b) – IFT pseudospectrum result for the frequency gap sequence (c), (d) – Convolution result of (a) and (b) pseudospectrums

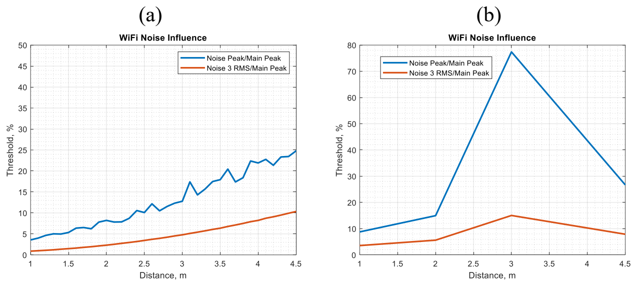

Fig. 10. Comparing simulation and experiment threshold for distance estimation under Wi-Fi noise: (a) – Simulation, (b) - Experiment

In the described above case, the power of Wi-Fi communication was similar to the BLE communication power. Assume the distance between the initiator and reflector increases, but the distance to the Wi-Fi source from one of the boards is the same. To find at what range will the distance estimation not work we build a simulation model, which is based on the following equations:

$$Z_1 = IQ_1 + W_1 + n_1\,, \tag{25}$$

$$Z_2 = IQ_2 + W_2 + n_2, \tag{26}$$

$$Z = Z_1 \cdot Z_2 = (IQ_1 + W_1 + n_1)(IQ_2 + W_2 + n_2\,), \tag{27}$$

where Z_1 and Z_2 are complex values at the initiator and reflector, respectfully, W_1 and W_2 represent the complex Wi-Fi noise, which differs only by the amplitude between the boards due to the free-space loss for different distances to the Wi-Fi source (Fig. 4). The result of the simulation shown in Fig. 9, help establish a threshold value, which is a ratio between the noise peak on the pseudospectrum and the main lobe amplitude. To compare, a line of 3 RMS was plotted, indicating the relative impact of the noise.

With high probability, the ranging would be impossible after 10-15 meters due to signal attenuation and interference. An experiment under similar conditions was done (Fig. 10b), limiting our measurements to a maximum distance of 4.5 meters. The error in distance estimation showed a predictable dependence on distance, with an exception at one outlier point. Additionally, there could be problems with the connection due to the considerable noise. While IQ measurement can be successfully made at frequencies outside Wi-Fi noise, problems with connection procedures are possible if all advertising frequencies are noisy

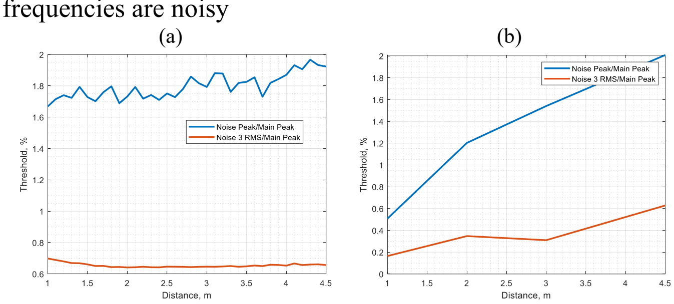

Fig. 11. Simulation and experiment results of excluding damaged frequencies from distance estimation: (a) – Simulation, (b) - Experiment

The effectiveness of BLE Phase-Based Ranging under Wi-Fi noise can be significantly increased if IQ data at damaged frequencies are multiplied by zero (Fig. 11), which is the easiest way to exclude damaged data from calculation (also known as "blocklisting").

The blocklisting sequence G_n may consists of binary values (1 and 0) or might assign weights for each channel based on the measured quality criteria. Unfortunately, this leads to an inability to use spatial smoothing techniques and, moreover, may adversely affect the impulse response. When a blocklist is applied new impulse response $\hat{h}_k^{(3)}$ is calculated as:

$$\hat{h}_k^{(3)} = \sum_{l=-\infty}^{\infty} \hat{h}_{k-l}^{(1)} g_l, \quad (28)$$

where:

$$g_l = \sum_1^N G_n \cdot exp\left(j \cdot 2\pi \cdot \frac{2d_k}{c} f_n\right), \quad (29)$$

is the blocklist impulse response. This means for some blocklist patterns with sidelobes in the transfer function, we will obtain false peaks in pseudospectrum (Fig. 12d). Another approach is to approximate damaged frequencies using neural networks or some other interpolation methods [21], though it can be less effective in dynamic environment.

In summary, mitigating Wi-Fi interference is a complex optimization task strongly dependent on the use case applications. For short-distance ranging, it works without special tricks. For long-distance ranging in static environments, interpolation could be a good choice. In dynamic environments and high distances, blocklisting may be a most effective choice, despite its drawbacks.

IV. CONCLUSIONS

This study underscores the significance of using Bluetooth Low Energy (BLE) wireless personal area network technology in IoT applications for indoor positioning and asset tracking, particularly in environments characterized by multipath propagation. While both the Inverse Fourier Transform (IFT) and Multiple Signal Classification (MUSIC) algorithms offer viable solutions for distance estimation, their effectiveness depends on factors like multipath interference and Wi-Fi noise. Wi-Fi interference presents a notable challenge, affecting the accuracy of Phase-Based Ranging (PBR) methods.

When used without spatial smoothing, MUSIC tends to be ineffective because the extreme points on its pseudospectrum are similar to those in the Inverse Furrier Transform pseudospectrum – the signal correlates within every ray, resulting in only one dominant eigenvalue. To increase MUSIC's performance in BLE PBR, spatial smoothing must be applied.

The ISM radio band, which BLE utilizes, is also shared by other communication technologies such as Z-Wave, ZigBee, and Wi-Fi, which can interfere with BLE. Fortunately, the behavior of this interference often resembles white noise caused by random packets at random time events. Generally, BLE PBR can accurately identify locations within 10 meters under Wi-Fi noise, even if the initiator or reflector is close to the router. The probability of such intense Wi-Fi noise is minimal in real-world environments. For IFT and MUSIC, the random ranging errors increase about 3-4 times without using additional correction algorithms and when Wi-Fi noise power is comparable to the signal power.

At the larger distances (greater than 10 meters) between the initiator and reflector, the WI-FI noise floor becomes comparable to the line-of-sight main lobes, resulting in significant ranging errors. In such cases, Wi-Fi noise attenuation becomes necessary. Typically, "blocklisting" channels are not scanned to avoid this interference, leading to transfer function modulation and the inability to apply spatial smoothing.

CREDIT AUTHORSHIP CONTRIBUTION STATEMENT

IK: Supervision, Conceptualization, Methodology, Data curation, Formal analysis, Writing – review & editing; **NK**: Investigation, Software, Formal analysis, Methodology, Writing – original draft; **OK**: Resources, Conceptualization, Visualization, Writing – review and editing; **AL**: Supervision, Validation, Visualization, Writing – original draft.

DATA AVAILABILITY

Data will be made available on request.

REFERENCES

[1] Number of Internet of Things (IoT) connected devices worldwide from 2019 to 2030, https://www.statista.com/statistics/1183457/iot-connected-devices-worldwide/; 2023 (accessed 13 May 2024).

[2] P. Barsocchi, M.G. Cimino, E. Ferro, A. Lazzeri, F. Palumbo, G. Vaglini, Monitoring elderly behavior via indoor position-based stigmergy, Pervasive and Mobile Computing. 23 (2015) 26–42. https://doi.org/10.1016/j.pmcj.2015.04.003

[3] X. Lu, Y. Yin, N. Zhao, H. Wei, 2021. Indoor positioning experiment based on phase ranging with Bluetooth low energy (BLE). Journal of Physics: Conference Series. 1971, e012044. https://doi.org/10.1088/1742-6596/1971/1/012044

[4] J. Wisanmongkol, L. Klinkusoom, T. Sanpechuda, L. Kovavisaruch, K. Kaemarungsi, Multipath mitigation for RSSI-Based bluetooth low energy localization. In 19th Inter. Symp. on Commun. and Inform. Technol. (ISCIT), 2019, p. 47–51. https://doi.org/10.1109/ISCIT.2019.8905164

[5] A.G. Abdellatif, A.A. Salama, H.S. Zied, A.A. Elmahallawy, M.A. Shawky, 2023. An improved indoor positioning based on crowd-sensing data fusion and particle filter, Physical Communication. 61, e102225. https://doi.org/10.1016/j.phycom.2023.102225

[6] Introducing RTT in Bluetooth https://www.bluetooth.com/specifications/specs/introducing-rtt-in-bluetooth-nwp/; 2019 (accessed 15 March 2024).

[7] G. Shen, R. Zetik, H. Yan, O. Hirsch, R.S. Thoma, Time of arrival estimation for range-based localization in UWB sensor networks. In IEEE Inter. Conf. on Ultra-Wideband, 2010, p. 1–4. https://doi.org/10.1109/ICUWB.2010.5614041

[8] W. Kluge, E. Sachse, Distance measurement between two nodes of a radio network. Mar. 2013, US Patent App. 13/849,166.

[9] P. Zand, J. Romme, J. Govers, F. Pasveer, G. Dolmans, A high-accuracy phase-based ranging solution with Bluetooth low energy (BLE). In IEEE Wireless Commun. and Network. Conf., 2019, p. 1–8. https://doi.org/10.1109/WCNC.2019.8885791

[10] E. Yuan, W. Qi, P. Liu, L. Wei, L. Chen, Ranging method for navigation based on high-speed frequency-hopping signal, IEEE Access.6 (2018) 4308–4320. https://doi.org/10.1109/ACCESS.2017.2787801

[11] P. Boer, J. Romme, J. Govers, G. Dolmans Performance of high-accuracy phase-based ranging in multipath environments. In Proc. IEEE Int. Conf. Vehicular Tech. Conf., 2020, pp. 1–5. https://doi.org/10.1109/VTC2020-Spring48590.2020.9128721

[12] R. Miesen, F. Kirsch, P. Groeschel, M. Vossiek, Phase based multi carrier ranging for UHF RFID. In IEEE Inter. Conf. on Wireless Inf. Tech. and Sys. (ICWITS), 2012, pp. 1–4. https://doi.org/10.1109/ICWITS.2012.6417821

[13] C. Gomez, J. Oller, J. Paradells, Overview and evaluation of bluetooth low energy: An emerging low-power wireless technology, Sensors. 12 (2012) 11 734–11 753. https://doi.org/10.3390/s120911734

[14] S. Sunny, J.V. John, T.J. Apen, Quadrature Detection Methods for FM Demodulation. In Third International Conference on Advances in Computing and Communications, IEEE, 2013, p 433-436. https://doi.org/10.1109/ICACC.2013.92

[15] Y. Schröder, D. Heidorn, L. Wolf, Investigation of Multipath Effects on Phase-based Ranging. In the International Conference on Indoor Positioning and Indoor Navigation (IPIN), IEEE, 2019, p. 1-8. https://doi.org/10.1109/IPIN.2019.8911817

[16] A. Dutt, V. Rokhlin, Fast Fourier transforms for nonequispaced data, SIAM Journal on Scientific Computing. 14 (1993) 1368-1393. https://doi.org/10.1137/0914081

[17] C. Knapp, G. Carter, The generalized correlation method for estimation of time delay, IEEE Transactions on Acoustics, Speech, and Signal Processing. 24 (1976) 320-327.
https://doi.org/10.1109/TASSP.1976.1162830

[18] A. Dey, A. Nandi, B. Basu, Gold-MUSIC based DOA estimation using ULA antenna of DS-CDMA sources with propagation delay diversity, AEU-International Journal of Electronics and Communications. 84 (2018) 162-170. https://doi.org/10.1016/j.aeue.2017.11.029

[19] W. Li, Z. Dong, Z. Liu, X. Gao, X. Li, D. Zhai, 2024. Kalman-filter based hierarchical channel estimation for RIS-aided mmWave communication systems. Physical Communication, e102404.
https://doi.org/10.1016/j.phycom.2024.102404

[20] T.J. Shan, M. Wax, T. Kailath, On spatial smoothing for direction-of-arrival estimation of coherent signals, IEEE Transactions on Acoustics, Speech, and Signal Processing. 33 (1985) 806-811. https://doi.org/10.1109/TASSP.1985.1164649

[21] A. Sheikh, J. Romme, J. Govers, A. Farsaei, C. Bachmann, Phase-Based Ranging in Narrowband Systems with Missing/Interfered Tones, IEEE Internet of Things Journal. 10 (2023) 15171-15185. https://doi.org/10.1109/JIOT.2023.326479